Q-Maps: A New Synoptic Data Product for Investigating Dynamic Coronal Connectivity

Xudong Sun[1], J. Todd Hoeksema[1], Yang Liu[1], Zoran Mikić[2], and Viacheslav Titov[2]

[1] Stanford University (*xudong@sun.stanford.edu*); [2] Predictive Science Inc.

The Squashing Factor *Q*

• An infinitesimal circle is mapped along a field line into an infinitesimal ellipse. The aspect ratio of the resulting ellipse defines the squashing factor, *Q*, of the flux tube surrounding the field line (Fig. 1).

• Magnetic null, separator, and separatrix have infinite *Q* due to discontinuity in field line mapping. Quasi-separatrix layers (QSLs) have finite high *Q*.

• High-Q regions are preferred sites for magnetic reconnection and thus play key roles in flare, CME and slow solar wind.

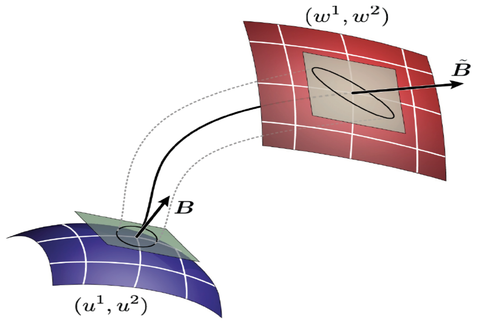

Fig 1 | Illustration of Q. The circle and ellipse are on the boundary surfaces of a finite volume defined by, for example, the photosphere and the source surface of a coronal field model (Titov+ 2009).

Uses of *Q*-Maps

• Identification of hyperbolic flux tubes as preferred sites for current sheet formation and thus **flare sites** (e.g., Savcheva+ 2012; Zhao+ 2014).

• Classification of **streamer & pseudo-streamer** as background environment which systematically affects CME speed (Liu 2007).

• Investigation of subtle magnetic linkage between remote regions that participate in **sympathetic eruptions** (Torok+ 2011, Titov+ 2012, Fig. 2).

• Visualization of **topological changes** related to eruptive/confined flares (Sun+ 2015, Fig. 3).

• Identification of **slow solar wind** source regions: the S-web model (Antiochos+ 2011, Titov+ 2011, Linker+ 2011).

• Visualization of flux tube expansion and empirical prediction of **solar wind speed** (Wang & Sheeley 1990, Arge+2000).

• **Evolution of magnetic topology** over days and over a solar cycle.

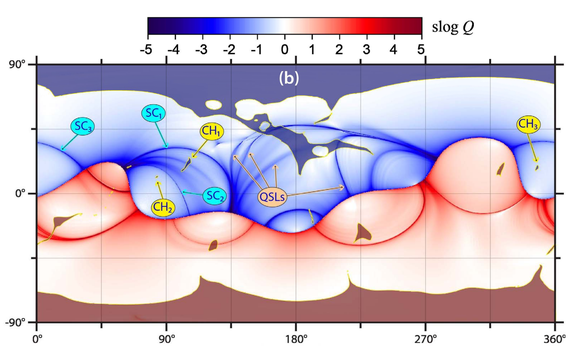

Fig 2 | Signed log-*Q* map of CR2099 for sympathetic events 2010-08-01 based on PFSS model. Red/blue colors indicate source-surface magnetic polarity. High-*Q* regions at that height are darker. Also plotted are coronal hole foot points at photosphere. Separatrix curtains (SC) of pseudo-streamers are easily seen (Titov+ 2012).

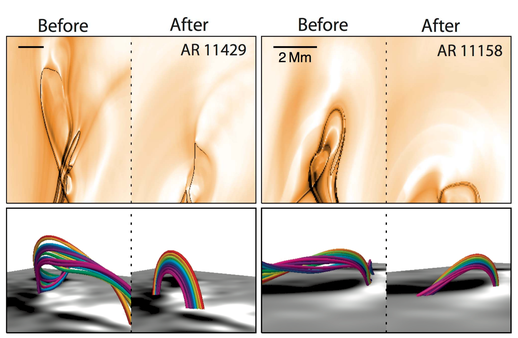

Fig 3 | Change of *Q* distribution after two eruptive flares based on NLFFF model. Top panels show *Q* maps on a vertical cross section in filament channels. The HFT/flux rope structure is clear. After the eruption such structure almost disappear. Lower panels show selected field lines that appear less twisted/sheared (Sun+ 2015).

Synoptic Data Product: *Q*-Maps Based on HMI/PFSS

• Routine coronal hole maps and *Q*-maps calculated on 10 different radial slices based on PFSS model and HMI data.

• Inputs: synoptic maps/synchronic frames corrected for polar field. Outputs: 0.25 deg maps per CR/per day.

• Code developed at Predictive Science Inc.; has been tested and ported to HMI pipeline.

• Routine and on-request runs; data and visualization available through JSOC and VSO.

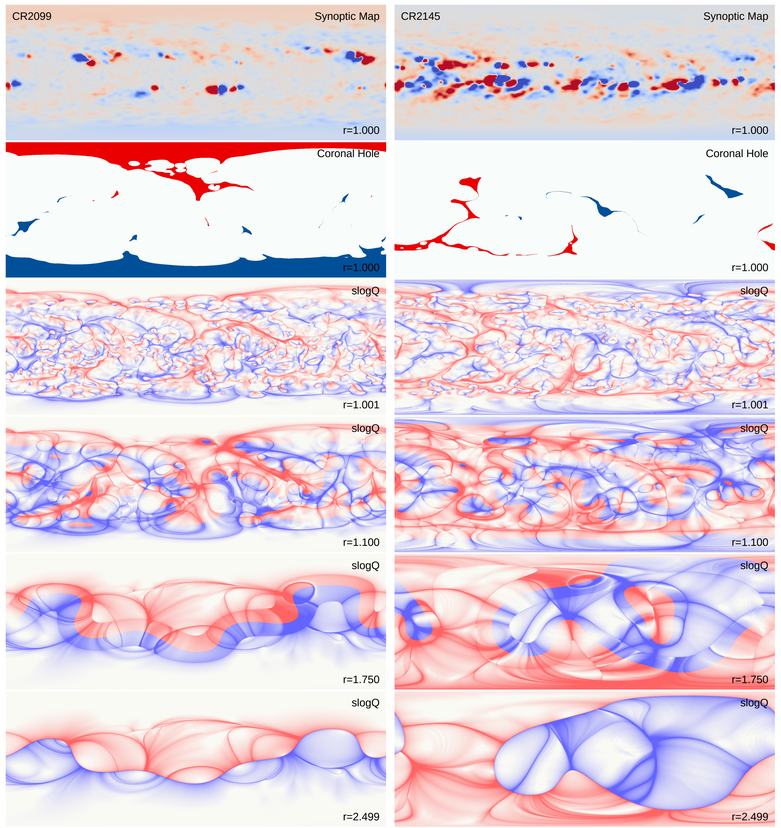

Fig 4 | Example output for CR2099 (left) and CR2145 (right). First row: input synoptic maps after smoothing, polar field correction, and re-meshing into a uniform latitude grid. Second row: coronal hole footpoint. Third to sixth rows: slog*Q* maps at 1.001, 1.10, 1.75, and 2.499 R. The complexity reduces drastically.

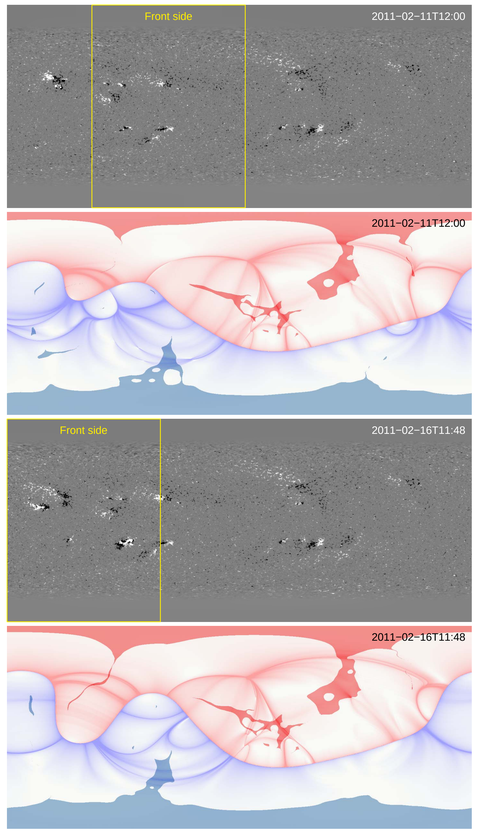

Fig 5 | Daily synchronic frames and signed log-*Q* maps of 2011 Feb 11 & 16. Emerging AR11158 and decaying bipoles in the north caused large topological changes.

Future Work

• Computing *Q* on routine and campaign MHD runs in comparison with the PFSS version.

• Active region *Q* maps using HMI vector data and non-potential extrapolation (e.g. Fig. 3).

• Possible auto-classification of topological structures.

• Visualization of data products (e.g., Fig 6).

Fig 6 | 3D rendering of the magnetic topology of CR2099. slog Q values on the source surface and the photosphere are rendered along with other topological structures (Titov+ 2012). Similar visualization is greatly helpful for understanding the coronal structure.